Electronic Supplementary Material (ESI) for CrystEngComm.
This journal is © The Royal Society of Chemistry 2018

Electronic Supplementary Information

Structural characterization of off-stoichiometric kesterite-type $Cu_2ZnGeSe_4$ compound semiconductors: From cation distribution to intrinsic point defect density

R. Gunder,[a] J. A. Márquez-Prieto[a], G. Gurieva[a], T. Unold[a] and S. Schorr[a,b]

Contents

Figure S1 WDX line scans averaged to proof the homogeneity of different CZGSe grains in a specific sample.

Equations S1 – S6 Calculation of sum formulae and defect type fraction exemplarily shown for an A/B-type mixture.

Figure S2 Refined XRD pattern of an off-stoichiometric G-F-type CZGSe sample containing ZnSe as secondary phase.

Figure S3 Unit cell volumes of off-stoichiometric CZGSe powder samples versus Cu/(Zn+Ge).

Figure S4 Refined neutron diffraction pattern of an off-stoichiometric, single-phase F-I-type CZGSe sample.

Figure S5 Total point defect concentration in dependence of the cation ratios.

Figure S6 Evolution of the stoichiometric coefficients of Cu, Zn, and Ge with changing Cu/(Zn+Ge).

Figure S7 Tauc plot of the diffuse reflectance data to deduce bandgap energies of CZGSe with different compositions.

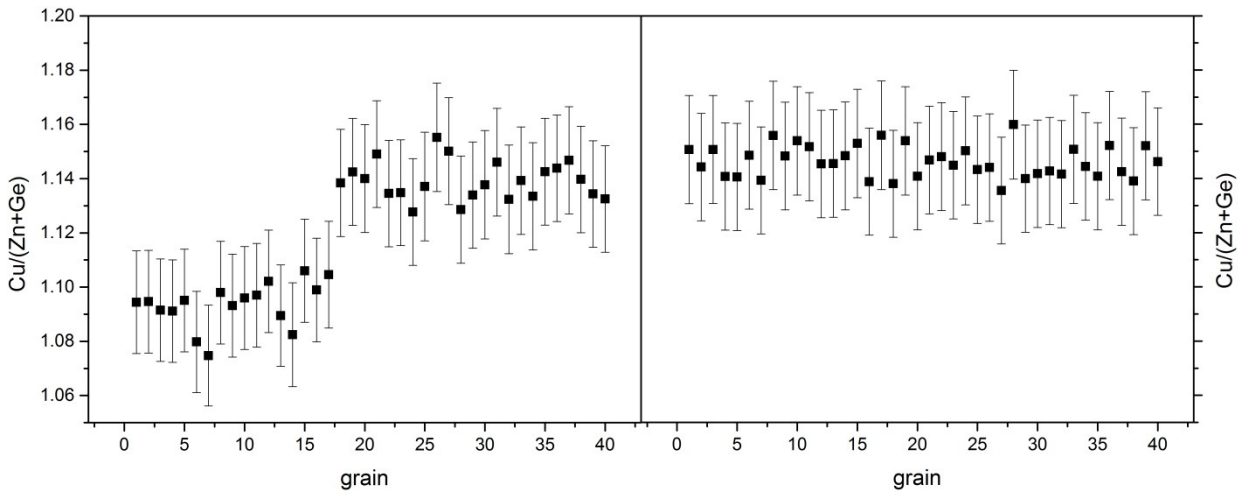

Figure S1 Averaged cation ratios obtained from WDX line scans for different grains of a C-type CZGSe sample. C-type samples heavily tend to form several kesterite phases after only one homogenization step (left panel). In some cases the repetition of homogenization step successfully led to the formation of a single kesterite phase (right panel).

The calculation of the sum formulae and the off-stoichiometry type fraction is exemplarily shown for A/B-type composition:

A-type

$$\frac{Zn}{Ge} = \frac{(1+a)}{1} \text{, solving for a delivers } a_y = \frac{Zn}{Ge} - 1 \qquad \text{(S1)}$$

$$\frac{Cu}{(Zn+Ge)} = \frac{(2-2a)}{(1+a+1)} \text{, solving for a delivers } a_x = \frac{(2-2a_y)}{(2+a_y)} \qquad \text{(S2)}$$

B-type

$$\frac{Zn}{Ge} = \frac{(1+3b)}{(1-b)} \text{, solving for b delivers } b_y = \frac{\left(\frac{Zn}{Ge} - 1\right)}{\left(\frac{Zn}{Ge} + 3\right)} \qquad \text{(S3)}$$

$$\frac{Cu}{(Zn+Ge)} = \frac{(2-2b)}{(1+3b+1-b)} \text{, solving for b delivers } b_x = \frac{(1-b_y)}{(1+b_y)}. \qquad \text{(S4)}$$

The type fraction is determined by linear interpolation between the two type lines adjoining the composition of a sample:

A-type:

$$A\,[\%] = \frac{\left(b_x - \frac{Cu}{(Zn+Ge)}\right)}{(b_x - a_x)} \cdot 100 \qquad \text{(S5)}$$

B-type:

$$B\,[\%] = \frac{\left(\frac{Cu}{(Zn+Ge)} - a_x\right)}{(b_x - a_x)} \cdot 100 \qquad \text{(S6)}$$

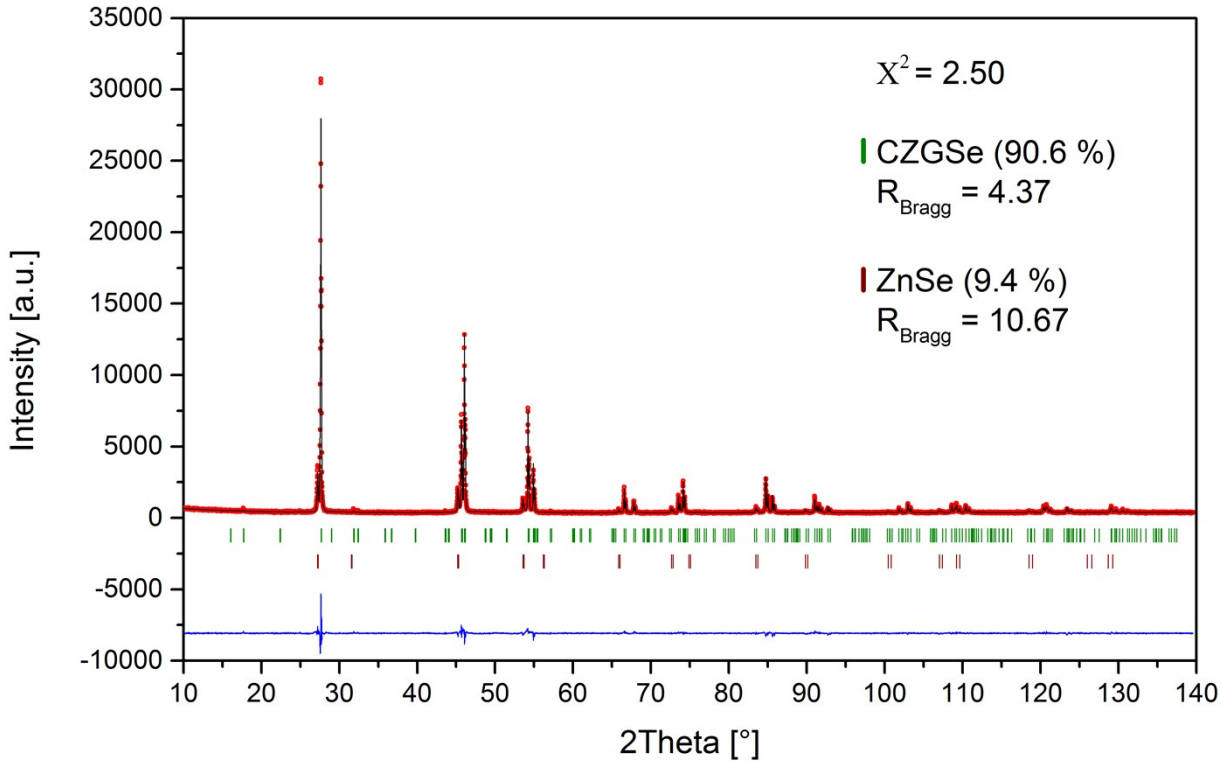

Figure S2 Refined XRD pattern of an off-stoichiometric G-F-type CZGSe sample containing ZnSe as secondary phase.

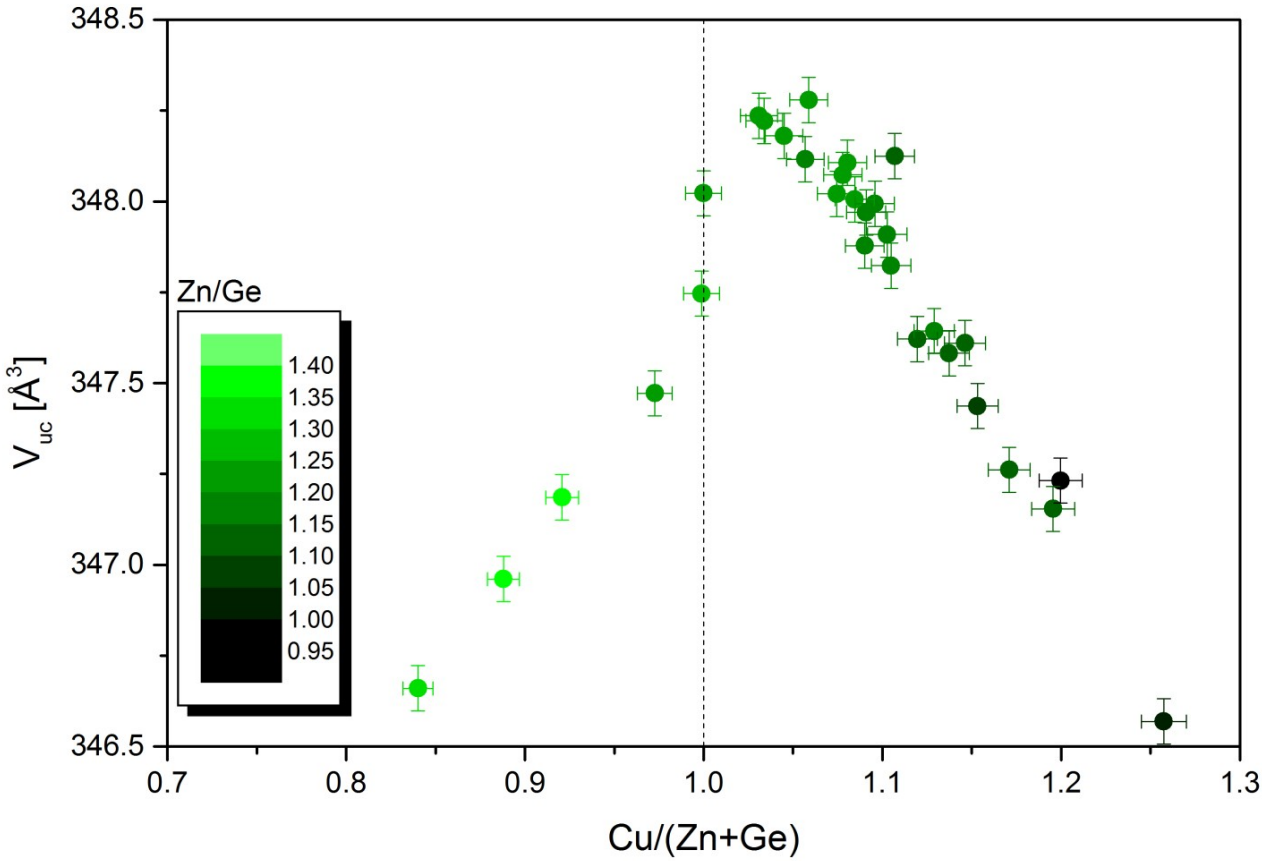

Figure S3 Unit cell volumes of off-stoichiometric CZGSe powder samples versus Cu/(Zn+Ge).

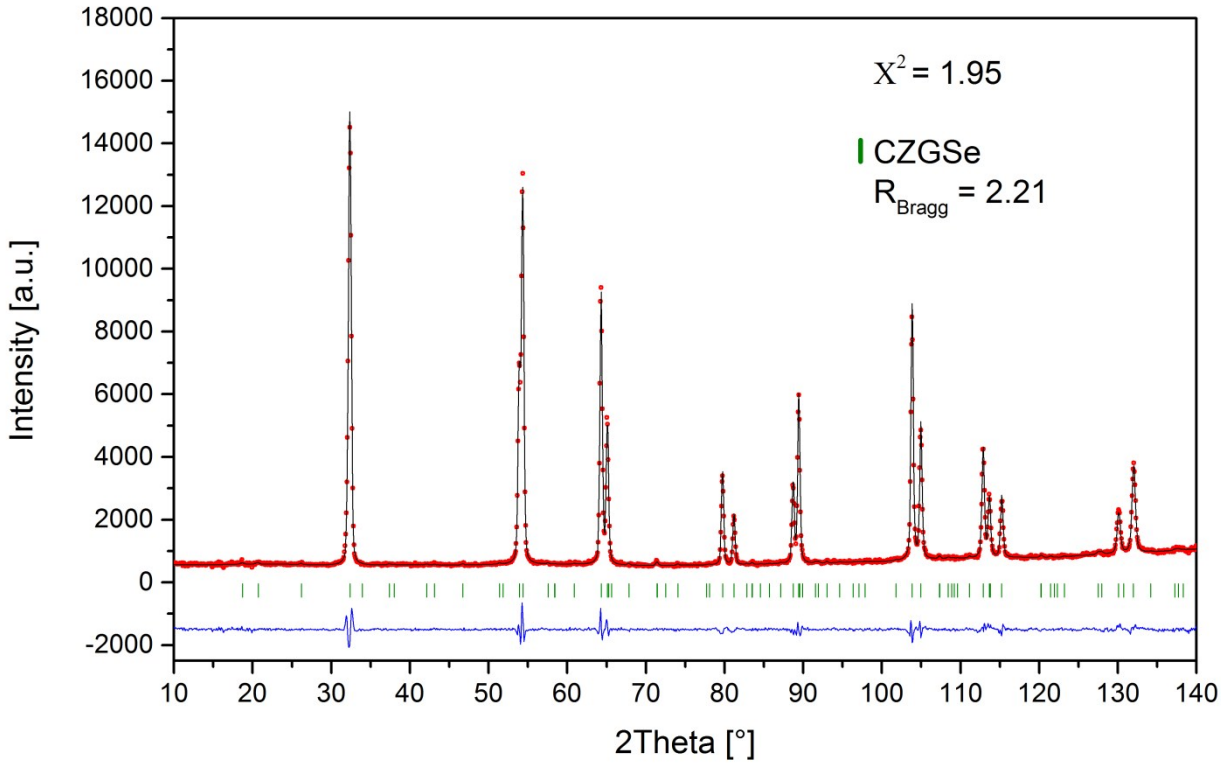

Figure S4 Refined neutron diffraction pattern of an off-stoichiometric, single-phase F-I-type CZGSe sample.

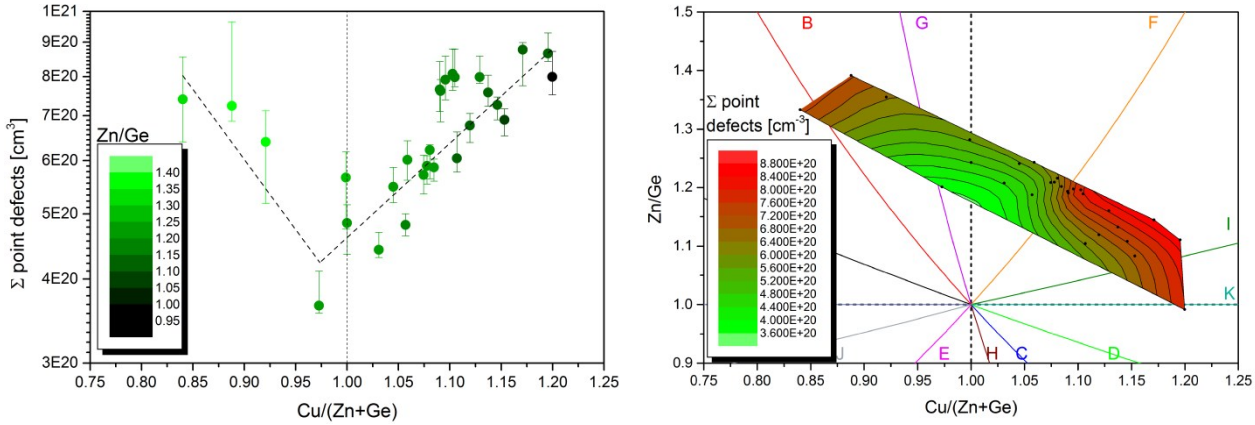

Figure S5 Overall point defect concentration in off-stoichiometric kesterite-type CZGSe powder samples in dependence of cation ratios (Cu/Zn disorder excluded; dashed lines are given as guides to the eyes).

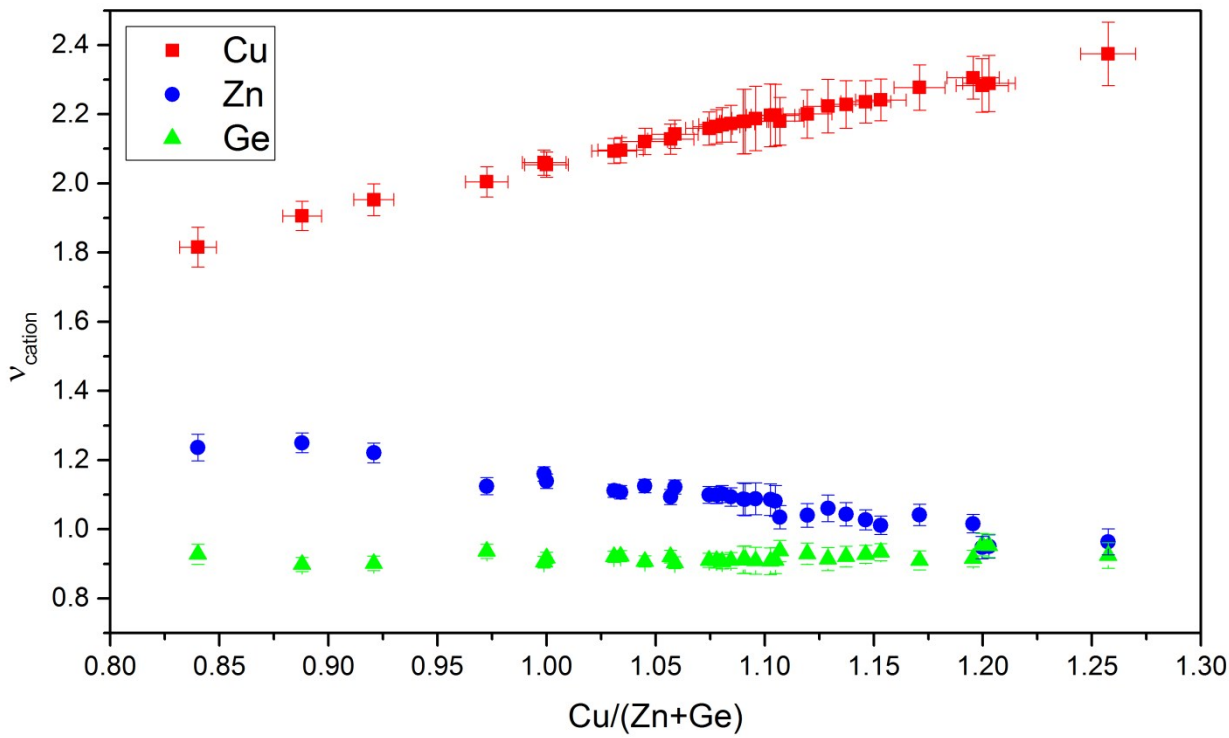

Figure S6 Evolution of the stoichiometric coefficients *v* of Cu, Zn, and Ge with changing Cu/(Zn+Ge).

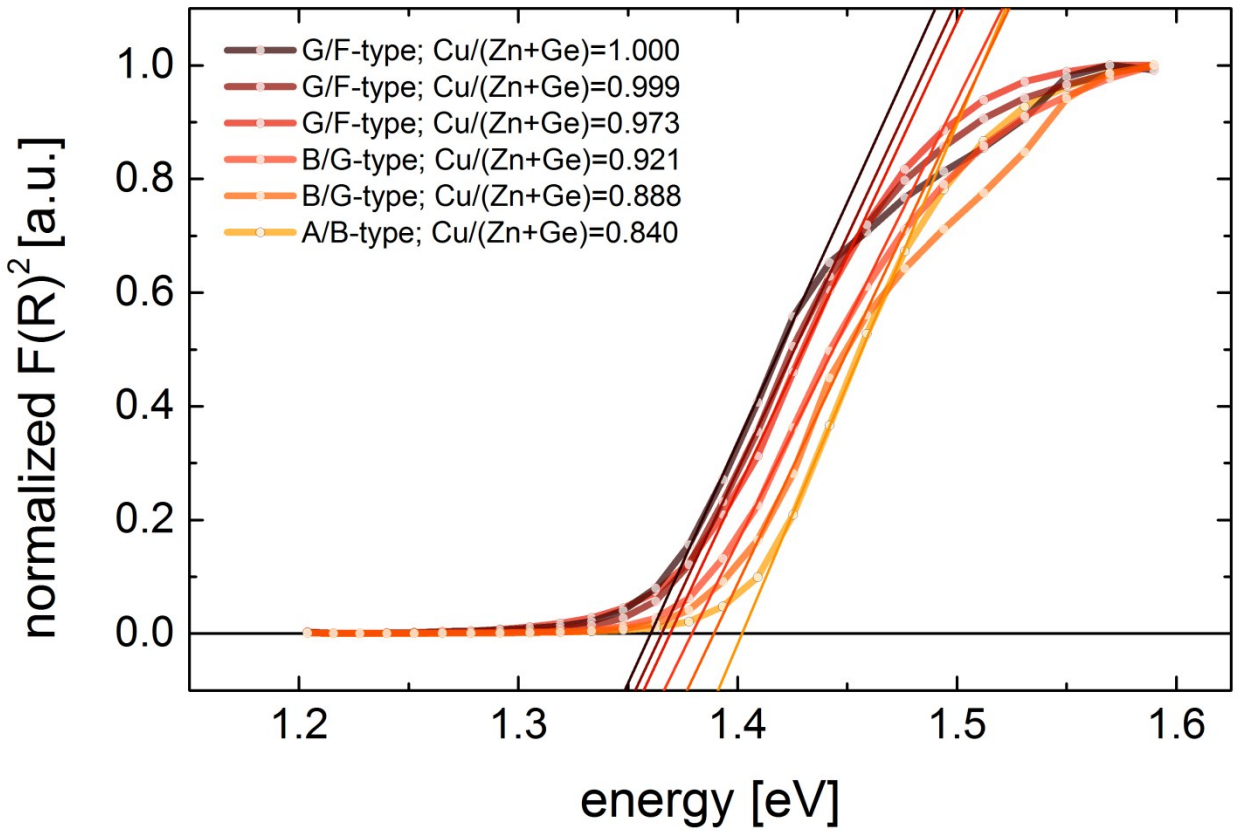

Figure S7 Tauc plot of the diffuse reflectance data to deduce bandgap energies of CZGSe with different compositions.